Understanding spaced-receiver zonal velocity estimation

B. M. Ledvina and P. M. Kintner
School of Electrical and Computer Engineering, Cornell University, Ithaca, New York, USA

E. R. de Paula
Divisão de Aeronomia/Ciências Espaciais e Atmosféricas, Instituto Nacional de Pesquisas Espaciais, São José dos Campos, São Paulo, Brazil

Received 19 March 2004; revised 3 August 2004; accepted 20 August 2004; published 27 October 2004.

[1] Spaced-receiver analysis can be used to estimate the ionospheric zonal irregularity velocity. This involves first measuring the scintillation pattern velocity and then estimating the zonal irregularity velocity. A straightforward technique involving projection planes has been used to derive a relationship between the satellite position and velocity, the irregularities' position and velocity, and the scintillation pattern velocity. This relationship relies on the alignment of the irregularities along the field lines but is independent of the irregularity spectrum. When simplified, this relationship can be used to estimate the zonal irregularity velocity using either geostationary satellites or Global Positioning System (GPS) satellites. This estimation is straightforward but must be performed in a careful manner. An example of zonal irregularity velocity estimation using GPS satellites is presented. The average zonal irregularity velocity is estimated over a 3-week period in March 2002 at São Luís, Brazil ($-3.59°$ dip angle). This hourly average velocity has been compared with the climatological radar observations from Jicamarca Observatory. The spaced-receiver zonal velocity agrees well (within ±8 m/s) with the radar's observations during postsunset hours. *INDEX TERMS:* 2439 Ionosphere: Ionospheric irregularities; 2437 Ionosphere: Ionospheric dynamics; 2494 Ionosphere: Instruments and techniques; 2415 Ionosphere: Equatorial ionosphere; *KEYWORDS:* scintillations, spaced receivers, equatorial ionosphere, GPS

Citation: Ledvina, B. M., P. M. Kintner, and E. R. de Paula (2004), Understanding spaced-receiver zonal velocity estimation, *J. Geophys. Res.*, *109*, A10306, doi:10.1029/2004JA010489.

1. Introduction

[2] The scintillation-based spaced-receiver technique has been used for decades to remotely sense properties of scattering mediums. The most common near-Earth medium is the *F* region ionosphere. In the equatorial region, the spaced-receiver technique is commonly used to estimate the zonal irregularity drift velocity [*Basu et al.*, 1991; *Valladares et al.*, 1996; *Basu et al.*, 1996; *Kil et al.*, 2000]. The technique has also been used to study the orientation and shape of irregularities in auroral regions [*Livingston et al.*, 1982; *Costa et al.*, 1988], and the velocity and orientation of scintillation patterns at the southern anomaly [*Kintner et al.*, 2004]. This paper examines using the spaced-receiver technique to estimate the zonal drift velocity of ionospheric irregularities.

[3] The spaced-receiver technique relies on radio wave diffraction by plasma density irregularities in the ionosphere. The source of the radio wave is typically an artificial satellite or a radio star. Diffraction produces amplitude and phase scintillation patterns that are sensed on the ground by the receivers. The movement of these patterns is, in the simplest approximation, a function of the irregularities' position and velocity and the satellite's position and velocity. Measuring the scintillation (diffraction) pattern velocity between two or more spaced receivers allows for estimation of the velocity of the irregularities. Irregularity velocity estimation requires understanding of the dynamics of the system. Note that in this paper the term ''scintillation pattern'' is used instead of ''diffraction pattern'', and that all references to scintillations are with regard to amplitude scintillations. Note that this does not preclude the use of phase scintillations for velocity estimation, but instead the topic is not investigated here.

[4] The zonal irregularity velocity is of interest because it relates to the underlying mechanisms in the ionosphere that are involved with generation and transport of irregularities. This velocity is easier to estimate than the vertical irregularity velocity due to satellite and receiver geometry.

[5] Previous work on spaced-receiver-derived zonal irregularity velocities has shown physically reasonable results [*Valladares et al.*, 1996; *Basu et al.*, 1991]. Validity comparisons are typically made with radar-derived results [*Basu et al.*, 1991] or airglow images [*Anderson and Mendillo*, 1983]. On numerous occasions, however, discrepancies between radar-derived zonal velocities and the scintillation-based zonal velocities have been noted [*Basu et al.*, 1996; *Kil et*

0148-0227/04/2004JA010489

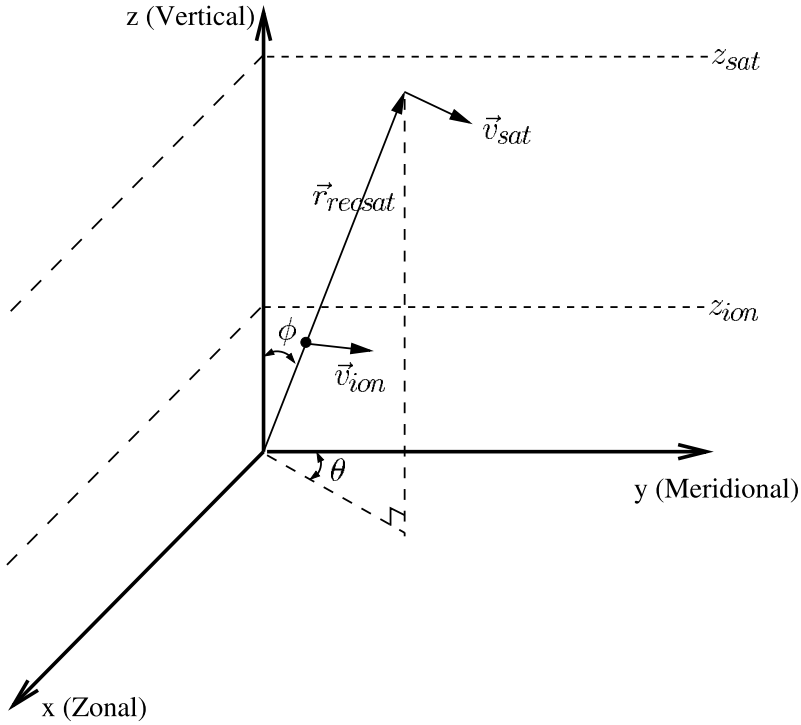

Figure 1. Illustration of the receiver coordinate system. The receiver coordinate system shows the satellite velocity vector, mean irregularity velocity vector, the satellite position vector, mean irregularity height, and angles between different vectors.

al., 2000]. In one situation, concurrent zonal irregularity velocities at the equator measured from one geostationary satellite to the east and another to the west were biased by approximately 20 m/s [*Basu et al.*, 1996]. The most striking discrepancy is found in *Kil et al.* [2000], where the scintillation-based zonal irregularity velocity at the southern anomaly was found to be, on average, 10–30 m/s larger than climatological radar results at the equator. The difference in locations is the most likely cause of the discrepancy. Regardless, it is not clear that the literature demonstrates a clear understanding of the relationship between the satellite position and velocity, irregularity position and velocity, and scintillation pattern velocity. To this end, the work presented here expands on previous work by deriving the general relationship of the system dynamics, by explaining how to estimate the zonal irregularity velocity for various satellite and receiver combinations, and by demonstrating experimental results.

[6] The remainder of this paper is organized in the following way. The second section reviews the spaced-receiver technique. The third section explains the details of measuring the scintillation pattern velocity. The fourth section discusses using either a geostationary satellite or GPS satellites for zonal irregularity velocity estimation. Section 5 presents a comparison with radar. Section 6 discusses the results. Section 7 provides a summary and concluding remarks.

2. Review of the Spaced-Receiver Technique

[7] The spaced-receiver technique is commonly used to either estimate the movement of scintillation patterns at the receivers or to estimate the properties of ionospheric plasma irregularities. The technique involves transmission of one or more radio waves from a remote source, which is typically an artificial satellite. The carrier frequency of the radio waves must be larger than the plasma frequency or electron gyrofrequency. The waves are diffracted by ionospheric irregularities of the appropriate Fresnel scale size embedded in a background plasma of significant density. Diffraction produces a scintillation pattern in amplitude and phase [*Yeh and Liu*, 1982]. Two or more receivers (typically on the ground) measure the velocity and orientation of this pattern. These measurements are commonly performed using cross-correlation [*Costa et al.*, 1988] or cross-spectral techniques [*Costa and Fougere*, 1988]. From the measurements, the irregularities' orientation, anisotropy [e.g., *Costa et al.*, 1988], and zonal velocity can be estimated [e.g., *Vacchione et al.*, 1987].

[8] A required component of spaced-receiver analysis is the definition of a local receiver coordinate system. A convienent local receiver coordinate system has its x axis aligned along the magnetic eastward (zonal) direction, its z axis coincides with the local vertical direction, and its y axis completes the right-hand coordinate system. This coordinate system, shown in Figure 1, has a receiver plane defined by the xy plane. The polar angle ϕ is the satellite zenith angle and θ is the satellite azimuth angle, which is defined clockwise with respect to magnetic north in the receiver coordinate system.

[9] It is assumed that the receivers are stationary and capable of precisely measuring and time tagging the received signal power. The satellite is allowed to be either stationary or moving. Both the receivers and the satellite

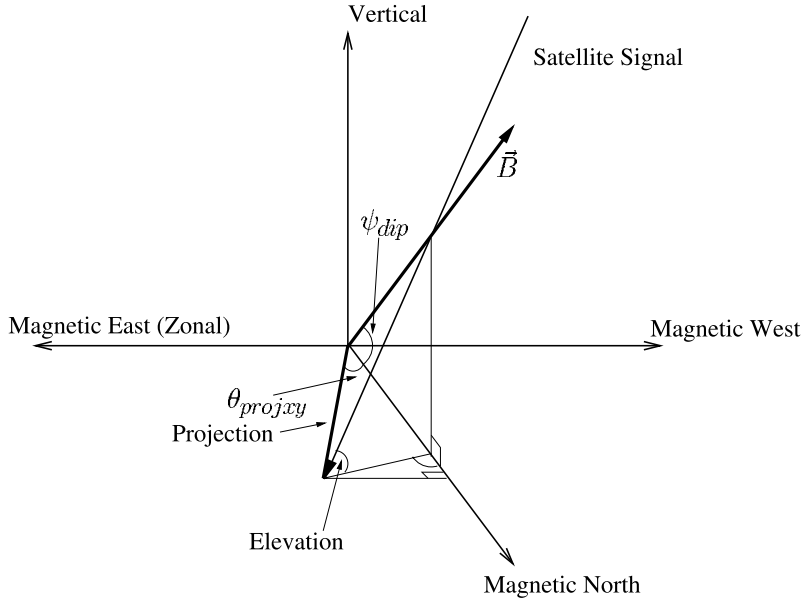

Figure 2. Illustration of scintillation pattern projection in the local receiver coordinate system. This illustration assumes that irregularities are aligned along the field lines. The scintillation pattern in the receiver plane is aligned along the projection.

should be sufficiently far from the scattering medium such that their relative distances are much greater than the scale size of the irregularities that cause diffraction. This condition, which is assumed here, is called Huygen-Fresnel diffraction. Note that this technique is not limited to the use of stationary receivers, but instead this assumption is made for simplicity.

[10] The propagation ray paths are assumed to be straight; that is they are not perturbed by changes in the index of refraction. The addition of refractive effects is beyond the scope of this paper, but would be a straightforward extension of this work. Additionally, the signal propagation speed, which is nominally the speed of light, is assumed to be much greater than the scintillation pattern velocity or satellite velocity.

[11] The scintillation-causing irregularities are assumed to occupy a relatively thin layer and to be aligned along the magnetic field lines [*Yeh and Liu*, 1982]. This alignment causes the scintillation pattern produced by the irregularities to be projected onto the receiver plane [*Rino and Livingston*, 1982; *Kintner et al.*, 2004]. The scintillation pattern projection is not necessarily aligned along the magnetic field direction. Figures 2 and 3 illustrate this idea.

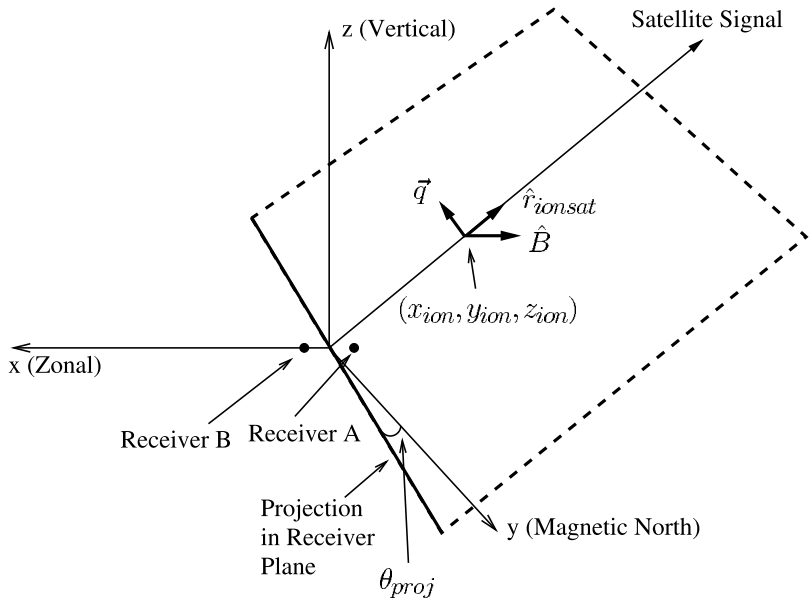

Figure 3. Illustration of the projection plane in the receiver coordinate system. This illustration complements Figure 2 by providing another view of the scintillation pattern projection.

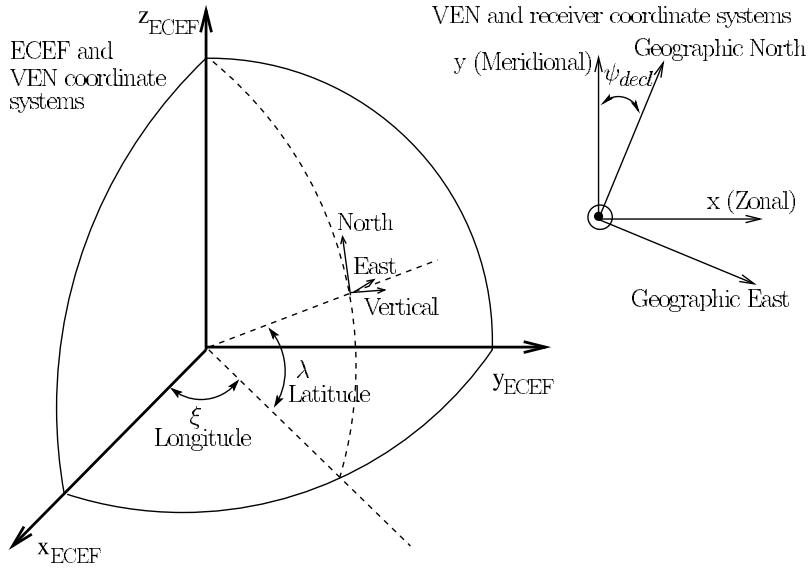

Figure 4. Illustration showing the ECEF, VEN, and receiver coordinate systems. The transformation from ECEF to VEN is a combination of two rotations by the geographic latitude and longitude. The rotation from VEN to the receiver coordinate system is a rotation by the negative of the declination angle about the vertical axis.

[12] The irregularities' magnetic field alignment and the signal ray path define a plane that contains the projected scintillation pattern. This plane, denoted here as the projection plane, is given by

$$\vec{q}^{\,\mathsf{T}}\vec{r}_{ionsat} = 0, \tag{1a}$$

$$\vec{q}^{\,\mathsf{T}}\hat{B}(\vec{r}_{ion}) = 0, \tag{1b}$$

where $\vec{r}_{ionsat}$ is the vector from the ionospheric puncture point to the satellite, $\hat{B}(\vec{r}_{ion})$ is the unit vector of the Earth's magnetic field at the ionospheric puncture point, $\vec{q}$ is the vector normal to these two former vectors, and the superscript T represents a vector transpose. The normal vector $\vec{q}$ is a function of the magnetic field direction at the ionospheric puncture point. All vectors are defined as 3×1 column vectors.

[13] The projection plane, defined by the normal vector $\vec{q}$, can also be written as

$$\vec{q}^{\,\mathsf{T}}(\vec{r} - \vec{r}_{ion}) = 0, \tag{2}$$

where $\vec{r}_{ion}$ is the position of the ionospheric puncture point and $\vec{r}$ is an arbitrary point in the projection plane.

[14] The velocity of the scintillation pattern in the receiver plane can be solved for by taking the partial time derivative of equation (2). This velocity in the zonal direction is (see Appendix A)

$$\begin{aligned} v_{scintx} = \frac{z_{sat}}{z_{sat} - z_{ion}} \{ & v_{ionx} + (q_y/q_x)v_{iony} \\ & + (q_z/q_x)v_{ionz} - \frac{z_{ion}}{z_{sat}}[v_{satx} + (q_y/q_x)v_{saty} \\ & + (q_z/q_x)v_{satz}]\}, \end{aligned} \tag{3}$$

where z_{sat} is the satellite height above the receiver plane, z_{ion} is the mean scattering height, v_{ionx} is the mean zonal irregularity velocity, v_{iony} is the mean meridional irregularity velocity, v_{ionz} is the mean vertical irregularity velocity, $\vec{v}_{sat}$ is the satellite velocity, and the ratios of the normal vector components q_y/q_x and q_z/q_x are functions of the satellite zenith angle, the satellite azimuth angle, the magnetic dip angle at the ionospheric puncture point, and the magnetic declination angle at the ionospheric puncture point. These two ratios are essentially mapping factors of the scintillation pattern (and its velocity) into the xy plane and xz plane. q_y/q_x and q_z/q_x are defined in Appendix A. The heights z_{ion} and z_{sat} generally do not coincide with the altitude above the Earth's surface. All quantities are defined in the receiver coordinate system.

[15] Equation (3) is expressed in such a way that it is clear how the satellite velocity (or ionospheric puncture point velocity) and the irregularities' drift velocity relate to the scintillation pattern velocity.

[16] Three rotation matrices are required to transform between different coordinate systems. The rotation matrix from the Earth-centered Earth-fixed (ECEF) coordinate system to a vertical, east, north (VEN) local coordinate system is

$$R_{VEN}(\lambda, \xi) = \begin{bmatrix} \cos(\xi)\cos(\lambda) & \sin(\xi)\cos(\lambda) & \sin(\lambda) \\ -\sin(\xi) & \cos(\xi) & 0 \\ -\cos(\xi)\sin(\lambda) & -\sin(\xi)\sin(\lambda) & \cos(\lambda) \end{bmatrix}, \tag{4}$$

where λ is geographic latitude and ξ is geographic longitude. See Figure 4 for an illustration of this transformation. This transformation, which is a combination of two rotations, is commonly used in navigation [*Hofmann-Wellenhof et al.*, 1994]. The rotation matrix for the transformation from the VEN coordinate system to the receiver coordinate system rotates about the local vertical

axis by the negative of the magnetic declination angle. It is given by

$$R_V(\psi_{decl}) = \begin{bmatrix} 1 & 0 & 0 \\ 0 & \cos(\psi_{decl}) & -\sin(\psi_{decl}) \\ 0 & \sin(\psi_{decl}) & \cos(\psi_{decl}) \end{bmatrix}, \quad (5)$$

where ψ_{decl} is the magnetic declination angle. When this rotation matrix is used to rotate into the receiver coordinate system, ψ_{decl} is nominally the magnetic declination at the origin of the receiver coordinate system.

[17] The rotation matrix that rotates about the zonal (eastward) direction by the negative of the dip angle in a local coordinate system is

$$R_E(\psi_{dip}) = \begin{bmatrix} \cos(\psi_{dip}) & 0 & \sin(\psi_{dip}) \\ 0 & 1 & 0 \\ -\sin(\psi_{dip}) & 0 & \cos(\psi_{dip}) \end{bmatrix}, \quad (6)$$

where ψ_{dip} is the magnetic dip angle.

[18] A combination of the above three rotations is needed to convert the estimated irregularity velocity $\vec{v}_{ion}$ into the zonal, vertical, and meridional velocities at the ionospheric puncture point. The transformation from the ionospheric velocities in the receiver coordinate system to the field-aligned coordinate system at the ionospheric puncture point is

$$\vec{v}_{ipp} = R\vec{v}_{ion}, \quad (7)$$

and

$$R = R_E(\psi_{dipipp}) R_V(\psi_{declipp}) R_{VEN}(\lambda_{ipp}, \xi_{ipp}) \cdot R_{VEN}^{-1}(\lambda_{rec}, \xi_{rec}) R_V^{-1}(\psi_{declrec}), \quad (8)$$

where $\vec{v}_{ipp}$ is the field-aligned irregularity velocity at the ionospheric puncture point, ψ_{dipipp} is the dip angle at the ionospheric puncture point, $\psi_{declipp}$ is the declination angle at the ionospheric puncture point, λ_{ipp} and ξ_{ipp} are the geographic latitude and longitude of the ionospheric puncture point, λ_{rec} and ξ_{rec} are the geographic latitude and longitude of the origin of the receiver coordinate system, and $\psi_{declrec}$ is the declination angle at the receivers. The subscripts *rec* and *ipp* are used to differentiate between angles associated with the receiver coordinate system and angles associated with the field-aligned coordinate system at the ionospheric puncture point, respectively. The superscript -1 denotes matrix inversion.

[19] The product of the two inverse rotation matrices in equation (8) is a transformation from the local receiver coordinate system to the ECEF coordinate system. The product of the three remaining rotation matrices transforms from the ECEF coordinate system to the field-aligned coordinate system at the ionospheric puncture point.

[20] It is instructive to give a simplified form of the transformation from the receiver coordinate system to the irregularity coordinate system. The only assumption is that the meridional irregularity velocity in the irregularity coordinate system is zero. This gives the following zonal and vertical irregularity velocities at the ionospheric puncture point:

$$\begin{bmatrix} v_{ippx} \\ v_{ippz} \end{bmatrix} = \begin{bmatrix} R_{11} - \frac{R_{21}R_{12}}{R_{22}} R_{13} - \frac{R_{23}R_{12}}{R_{22}} \\ R_{31} - \frac{R_{21}R_{32}}{R_{22}} R_{33} - \frac{R_{23}R_{32}}{R_{22}} \end{bmatrix} \begin{bmatrix} v_{ionx} \\ v_{ionz} \end{bmatrix}, \quad (9)$$

where the components of R in equation (8) have been used, and the subscripts indices are row then column. The components' explicit expressions are not shown here because they are straightforward to calculate and are not used in the remainder of this paper.

[21] One application of the spaced-receiver technique measures the velocity on the left-hand side of equation (3) and estimates the zonal irregularity velocity in the receiver coordinate system, v_{ionx}. For the most part, the literature discusses this velocity instead of the zonal velocity at the ionospheric puncture point. This is because the zonal velocity at the ionospheric puncture point is, in general, a function of the vector velocity $\vec{v}_{ion}$, and the nonzonal components of this vector are difficult to estimate. To this end, investigating the estimation of v_{ionx} is the focus of the remainder of this paper.

3. Measuring the Scintillation Pattern Velocity

[22] The scintillation pattern velocity is the primary observable in spaced-receiver analysis. This velocity is the basis for estimating the irregularities' dynamics. The velocity of the scintillation pattern in equation (3) is defined at a single point in the receiver plane, however, measurement of the velocity is typically performed at two closely spaced points (on the order of the Fresnel distance) in the receiver plane. Spaced-receiver analysis estimates the scintillation pattern velocity by dividing the receivers' separation distance by the scintillation pattern time lag between the two receivers. This measurement method is reasonable, as long as it is assumed that the scintillation pattern velocity is constant during the time lag. In fact, it must be assumed that the velocity of the scintillation pattern is constant during the time history used to compute Fourier transforms or cross-correlation curves from which the time lag is derived. These data time histories are typically on the order of 30–90 s, forcing the assumption that the scintillation pattern velocity is constant during this latter time span.

[23] The estimate of the zonal scintillation pattern velocity using a pair of receivers may be biased with respect to the "truth" scintillation pattern velocity. Three different factors can lead to biases in the measured scintillation pattern velocity. First, if the scintillation pattern is evolving in time as it moves between receivers, the measured velocity is not the actual velocity of the scintillation pattern [*Briggs et al.*, 1950, 1968]. *Briggs et al.* [1950] demonstrated this and formulated a simple method to compensate for the decorrelation. Their "full correlation method" uses the measured zonal scintillation pattern velocity along with the assertion that the correlation functions are elliptical near their maximums to calculate both the true velocity of the scintillation pattern and its random or characteristic velocity.

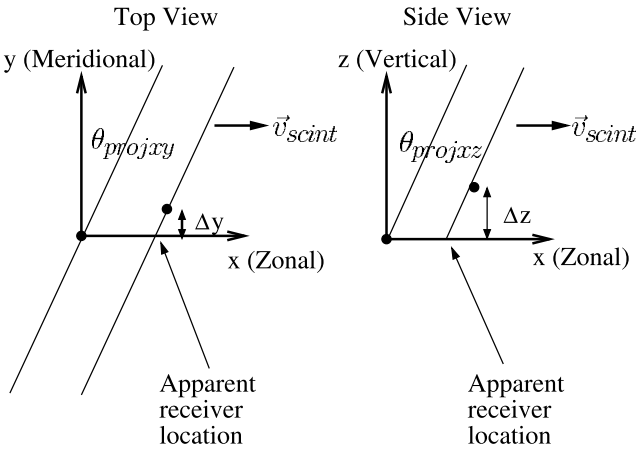

Figure 5. Illustration of the effects of misaligned receivers in the receiver coordinate system. Misalignment with respect to height and the magnetic meridian can produce biases in the measurement of the scintillation pattern velocity.

Several other authors have demonstrated more elaborate methods of dealing with evolving scintillation patterns [*Rino and Livingston*, 1982; *Vacchione et al.*, 1987; *Spatz et al.*, 1988; *Costa et al.*, 1988]. Their results are typically similar to those of *Briggs et al.* [1950].

[24] Second, the measured zonal scintillation pattern velocity may be biased if the receivers are not precisely aligned along the zonal direction (x axis). Note that it is important to position the receivers as close as possible along the zonal direction in order to precisely measure the zonal velocity. Deviations from the zonal direction can be corrected as long as the scintillation pattern's orientation does not coincide with the vector between the receivers. In this case the measured velocity is infinite, which is obviously not correctable.

[25] The zonal velocity measurement bias has two components related to the deviation within and orthogonal to the receiver plane. A displacement within the receiver plane along the meridional axis is a function of the scintillation pattern projection angle in the xy plane. A vertical displacement between the receivers produces a scintillation pattern velocity bias that is a function of the scintillation pattern projection angle in the xz plane.

[26] Figure 5 illustrates these biases. With these biases, the corrected scintillation pattern zonal velocity is

$$v'_{scintx} = v_{scintx}\left[1 - \frac{\Delta y \tan\left(\theta_{projxy}\right) + \Delta z \tan\left(\theta_{projxz}\right)}{d}\right], \qquad (10)$$

where the prime indicates the corrected velocity, d is the zonal receiver separation, Δy is the receivers' relative displacement within the receiver plane along the y axis, Δz is the receivers' relative vertical displacement from the receiver plane, θ_{projxy} is the projection angle in the xy plane, d is the receiver separation distance along the x axis (zonal) direction, and θ_{projxz} is the projection angle in the xz plane. These latter two angles are defined in Appendix A. Equation (10) was derived using trigonometry and the diagram in Figure 5.

[27] The third bias is denoted here as a cross-correlation "windowing effect." Cross-correlation of two scintillation pattern time histories over a finite interval causes apparent decorrelation. This is due to the fact that the two scintillation patterns at two spaced receivers for the same finite time span are typically not the same. A simple cross-correlation iterative technique eliminates the windowing effect. The iterative technique involves computing the cross-correlation function, shifting one data set by the optimal cross-correlation lag time, and repeating the process. Typically, two iterations are adequate for computing the maximally correlated optimal lag time. This approach is particularly useful when the scintillation pattern is evolving in time (i.e., the characteristic velocity is nonzero), receiver noise is significant, or the scintillations are weak.

[28] The range of observable scintillation pattern velocities has both lower and upper limits. The upper limit is dependent on the ratio of the receiver separation distance to the signal power sampling time interval. The lower limit is more complicated to quantify, but is to the first order limited by the ratio of the receiver separation distance to the data time span used to compute the cross correlation. The truth is that the lower limit is also dependent on the noise in the signal power time history and the lower limit for the cross-correlation peak that quantifies significant correlation. Assuming that these effects are no greater than one half the correlation time span, the following bounds can be derived:

$$\frac{d}{0.5t_{corr}} \le v_{scint} \le \frac{d}{\Delta t_{samp}}, \qquad (11)$$

where t_{corr} is the data time history length and Δt_{samp} is the data sampling interval. For example, if t_{corr} is 30 sec., Δt_{samp} is 0.02 sec., and the separation distance is 200 meters, the measurable scintillation pattern velocity is between 13.33 m/s and 10,000 m/s.

4. Estimating Zonal Irregularity Velocity

[29] The goal is to estimate the zonal irregularity velocity from the scintillation pattern velocity. In essence, the problem comes down to measuring the zonal scintillation pattern velocity and then solving equation (3) for the zonal irregularity velocity.

[30] Three unknowns exist in equation (3); the zonal irregularity velocity, v_{ionx}, the vertical irregularity velocity, v_{ionz}, the mean scattering height, z_{ion}. The dip angle at the ionospheric puncture point can be determined most accurately using a magnetic field model, such as the IGRF model, but only if z_{ion} is known. v_{iony} is assumed to be zero, which is allowable because of the long correlation distance along the field lines and the assumption that the differences in the field-aligned coordinate system and the receiver coordinate system are small. This under-determined equation cannot be solved analytically. Fortunately, methods to reduce the number of unknowns exist. The number of unknowns can be reduced in two ways. The first method is to use a geostationary satellite. The second method is to use a network of satellites and average the scintillation pattern velocity over a significant amount of time. These

two methods of variable reduction are investigated in this section.

4.1. Geostationary Satellite Case

[31] A convenient approach to estimating the zonal irregularity velocity is to use a geostationary satellite. These satellites are seen over a large portion of the Earth and can estimate the zonal irregularity velocity in the same location from day to day. A great deal of literature has been published that contains spaced-receiver experiments with geostationary satellites, particularly at sites in South America [e.g., *Valladares et al.*, 1996; *Basu et al.*, 1996; *Groves et al.*, 1997; *Bhattacharyya et al.*, 2001], Japan [e.g., *Karasawa et al.*, 1985], and India [e.g., *Ramo Rao et al.*, 2000].

[32] For a geostationary satellite, the scintillation pattern velocity (3) has a simplified form:

$$v_{scintx} = v_{ionx} + \left(q_y/q_x\right)v_{iony} + \left(q_z/q_x\right)v_{ionz}, \tag{12}$$

where the assumptions $z_{sat} \gg z_{ion}$ and $|\vec{v}_{sat}| = 0$ have been used. With two additional assumptions, equation (12) can be reduced to a simpler form. First, assume that the field-aligned coordinate system coincides with the receiver coordinate system, giving $B_x/B_y = 0$ and $B_z/B_y = \tan(\psi_{dip})$. Second, assume that $v_{iony} = 0$, which is nominally correct because of the large irregularity coherence along the field lines and the previous assumption. The simplified form is

$$v_{scintx} = v_{ionx} - \left[\frac{\tan(\phi)\sin(\theta)}{1 - \tan\left(\psi_{dip}\right)\tan(\phi)\cos(\theta)}\right]v_{ionz}, \tag{13}$$

where ψ_{dip} is the magnetic dip angle at the origin of the receiver coordinate system. This simplified form of the scintillation pattern velocity has been presented in numerous works [*Spatz et al.*, 1988; *Valladares et al.*, 1996], but they typically ignore the term with the magnetic dip angle.

[33] Referring to the simpler form of the scintillation pattern velocity, a spaced-receiver experiment using a geostationary satellite measures a scintillation pattern velocity that contains both the zonal and vertical irregularity velocities. Since the zonal velocity is typically of interest, the mapping of the vertical velocity into the scintillation pattern velocity is a nuisance. The mapping can be reduced by minimizing the term $\tan(\phi)$. This term is minimized by choosing a receiver location that is on the same magnetic longitude as the satellite. The least favorable geometry is that of a satellite directly magnetically east or west of the receiver, which ironically is a common location in much of the literature.

4.2. Averaging Using GPS Satellites

[34] The second way to reduce the unknowns in the equation (3) is by averaging. This is a good approach when a number of satellites, with arbitrary positions and velocities are available (e.g., GPS satellites). Averaging over all the scintillating satellites, over several days, over time tends to reduce the geometrical effects of the vertical irregularity velocity mapping and the unknown scattering height.

[35] The average zonal irregularity velocity is given by

$$\hat{v}_{ionxavg} = \sum_{i=1}^{N}\sum_{j=1}^{n_i}\sum_{k=1}^{n_j}\hat{v}_{ionxijk}, \tag{14}$$

where $\hat{v}_{ionx}$ is an estimate of the zonal irregularity velocity found by solving equation (3), estimating the scattering height, and setting the vertical irregularity velocity to 0, N is the number of days, n_i is the number of scintillating satellites, n_j is the number of samples to average over, the subscript i is a day index, subscript j is the satellite index, subscript k is a sample index, and the circumflex indicates an estimate.

[36] A mean scattering height must be assumed in order to compute the average zonal irregularity velocity. A well-accepted, although assumed, mean scattering altitude in the equatorial and midlatitude ionosphere is 350 km, which corresponds to the assumed F peak height during equatorial spread F events. Using this value in equation (14) implies that the mean scattering altitude over the averaging interval is 350 km, which is more reasonable than assuming that the instantaneous mean scattering altitude is 350 km. For example, a mean scattering altitude of 350 km is equal to a mean scattering height of 343.81 km if the satellite zenith angle is limited to 40 degrees.

[37] Over a long time span, the GPS satellites tend to be evenly distributed in the sky, particularly for receivers at low latitudes. This distribution has a mean value of $\tan(\phi)$ that can be quite small, particularly if satellites of significantly high elevation are used and several satellite signals are scintillating at any given time. A small mean value of $\tan(\phi)$ de-emphasizes the vertical irregularity velocity, allowing it to be ignored.

[38] Neglecting the terms that contain $\tan(\phi)$ and using an assumed mean scattering height of 343.81 km, leaves the following form for the average zonal irregularity velocity estimate:

$$\hat{v}_{ionxavg} \approx 0.9828 v_{scintxavg} + 0.0172 v_{satxavg}, \tag{15}$$

where $\hat{v}_{vionxavg}$ is essentially the average zonal irregularity velocity at zenith.

[39] Equation (15) states that the average zonal irregularity drift velocity is the average zonal scintillation pattern velocity plus the average ionospheric puncture point velocity. Equation (15) is similar to the equation used by *Kil et al.* [2000] to estimate the average zonal irregularity velocity at the southern equatorial anomaly using GPS satellites. The main difference in this result and theirs is that their coefficient preceding the scintillation pattern velocity is 1. This approximation adds a bias of 1–2 m/s in their estimate. Additionally, it is unclear how the ionospheric puncture point velocity was calculated in *Kil et al.* [2000].

5. Equatorial Example

[40] The average zonal irregularity velocity is computed at an equatorial location and compared with the climatological radar zonal drift velocity. The data set consists of GPS L1 amplitude scintillation data collected in São Luís, Brazil ($\psi_{dip} = -3.5°$, $\psi_{decl} = -20.8°$) during March 2002.

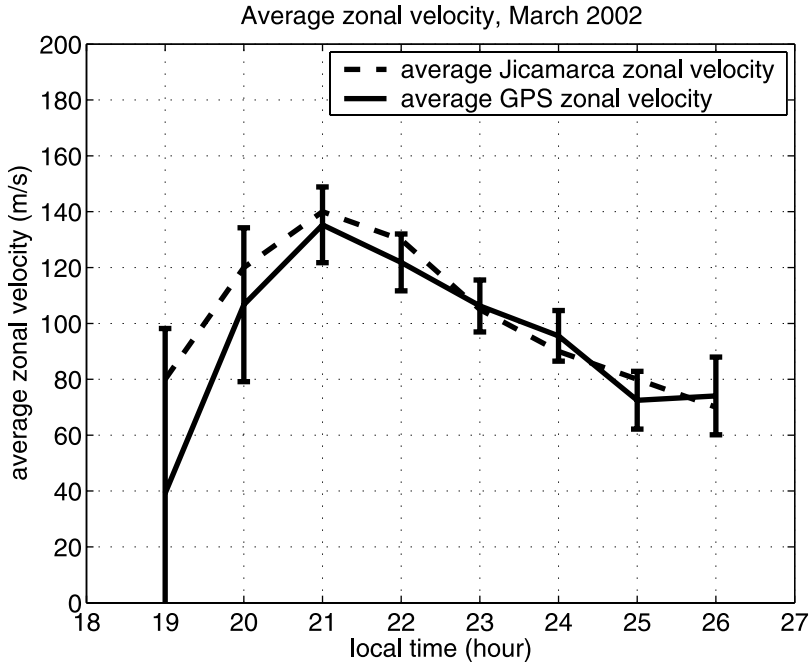

Figure 6. Comparison between seasonal zonal drift velocity from Jicamarca Radio Observatory [*Fejer et al.*, 1981] and the average zonal irregularity velocity from GPS spaced-receiver measurements. Local time lags UTC by 3 hours.

The data was collected using a pair of GPS L1 (1.57542 GHz) scintillation receivers that were designed at Cornell University [*Beach and Kintner*, 2001]. These receivers measure and record 50 Hz wideband power on the GPS L1 signal broadcast from the GPS satellites.

[41] The satellite signal power time histories are processed in the following way. For each scintillating signal with an S_4 index greater than or equal to 0.15, the autocorrelation and cross-correlation functions between two zonally spaced receivers are computed over successive 30-s intervals (1500 samples). The S_4 index cutoff has been used to minimize effects of multipath. Additionally, an elevation mask of 50 degrees (zenith mask of 40 degrees) has been used. The cross-correlation function is computed using two signal power time histories that span the same UTC time intervals. A minimum normalized coherence limit of 0.4 is used to retain only significantly correlated time histories.

[42] The 3-week average zonal irregularity velocity has been computed using data from 12 days in March 2002 that have significant scintillation activity. Figure 6 shows the average zonal drift velocity computed using the GPS spaced-receiver data. This result is compared with climatological results from Jicamarca Radio Observatory courtesy of *Fejer et al.* [1981]. Error bars on the spaced-receiver plot indicate the hourly standard deviation of the estimate. The largest uncertainty and variability in the zonal velocity occurs during the onset of scintillations, when the number of scintillating satellites is typically small, generally to the east of the receivers (personal observation, 2002), and the largest characteristic velocities occur. The large characteristic velocity may imply a shear in the zonal irregularity velocity or presence of large vertical velocities [*Pingree and Fejer*, 1987; *Wernik et al.*, 1983].

[43] It is not known if the assumed mean scattering altitude of 350 km is completely accurate. To this end, it is informative to compute the residual error between the estimate of the zonal velocity with a 350-km altitude and the estimate with another altitude. Figure 7 shows the computed residual error between the estimate in Figure 6 and a zonal velocity estimate using either a 300-km or a 450-km mean scattering altitude. The zonal velocity estimation in equation (15) is linear in z_{ion}, which explains the similarities in the residual error curves. The peak residual error in Figure 7 is -7 m/s, which indicates the zonal velocity estimation error does not vary dramatically with changes in the assumed mean scattering altitude. This is only true in an average sense.

6. Discussion

[44] The results presented in the previous section illustrate two important points. First, the zonal irregularity velocity can be estimated using either geostationary or GPS satellites. In the geostationary satellite case, the satellite and receiver geometry must be chosen to minimize the effects of the vertical irregularity velocity. When using GPS satellites, the average zonal irregularity velocity can be determined for a given time period.

[45] The second result is that the average zonal irregularity velocity is consistent with climatological results from radar. The largest deviation between the two occurs at the onset of scintillations, but tapers off after the first hour (20:00 local time) to being within 10 m/s of the radar's results. This good agreement is partly due to the lack of day-to-day variability of the zonal irregularity velocity (personal communication, David Hysell, 2003).

[46] It is unclear if the radar and spaced-receiver zonal velocities are directly comparable, particularly in an instan-

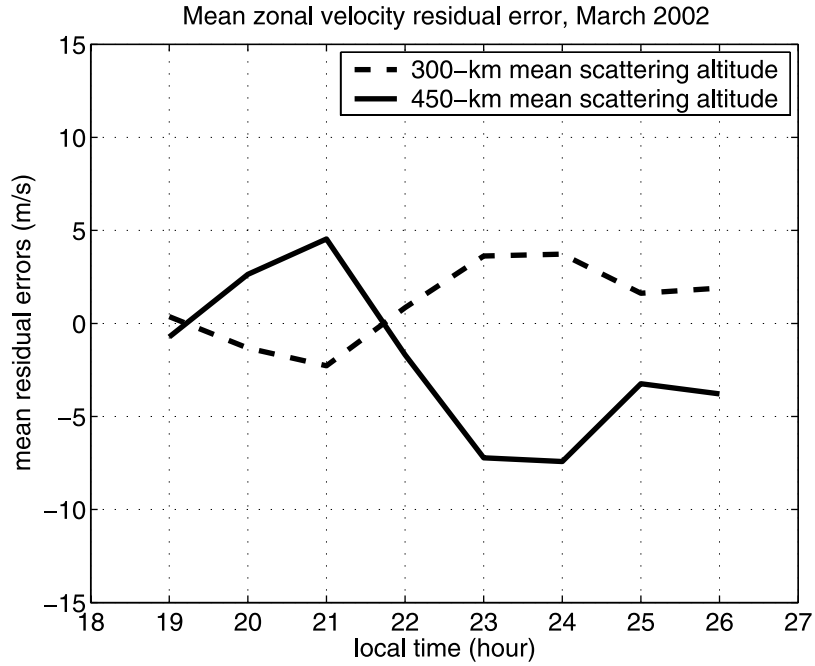

Figure 7. Hourly mean residual error of the zonal irregularity velocity associated with either a 300-km mean scattering altitude or a 450-km mean scattering altitude. The residual error is with respect to the estimate in Figure 6.

taneous sense. Several factors support this assertion. First, the two methods sense irregularities of different scale sizes, which may be experiencing different dynamics. Second, the integration method used to produce the climatological radar zonal velocities may be over a range of heights that does not correspond to the location of the irregularities causing scintillations. Third, the equatorial spread *F* ionosphere may exhibit different dynamics than the quiescent ionosphere.

[47] *Kil et al.* [2000] demonstrated a zonal irregularity velocity at the southern anomaly that was, on average, 10–30 m/s larger than the climatological results. Three reasons for the relatively large difference are possible. First, the spaced-receiver zonal irregularity velocity and radar zonal drift velocity may not be directly comparable, as mentioned above. Regardless, several authors have demonstrated good results comparing radar-derived drifts to spaced-receiver drifts [*Basu et al.*, 1991; *Valladares et al.*, 1996]. Second, the technique used to estimate the zonal velocity may be incorrect. This is unlikely since the equation relating the scintillation pattern velocity, satellite velocity, and irregularity velocity shown in *Kil et al.* [2000] is similar to results derived here. The third reason is that the average zonal irregularity velocity at the anomaly may be larger than at the equator. Experimental evidence of this has been shown by *Aggson et al.* [1987]. They used in situ electric field measurements from the DE 2 satellite to infer the average zonal drift velocity at a 300-km altitude. Their results indicate that the peak average zonal drift velocity of 200 m/s occurs at ±8° from the magnetic equator. The average zonal drift velocity at the equatorial anomalies was between 130–170 m/s, barring experimental error. At the equator a smaller zonal velocity was measured; however, it was considerably smaller than the spaced-receiver-derived results. This may be due to the relatively low altitude of the satellite. Regardless, if the spaced-receiver average zonal irregularity velocity follows a similar trend, the results of *Kil et al.* [2000] seem more plausible.

[48] Using data from 1999, *Kil et al.* [2002] also showed the GPS-derived mean zonal irregularity velocity at São Luís. Their velocity was on average larger than the velocity show in Figure 6. This result suggests a seasonal variation of the zonal velocity that may be a function of the solar cycle. Radar-derived zonal velocities tend to be maximum at the peak of the solar cycle [*Fejer et al.*, 1981], suggesting that a similar pattern may exist in spaced-receiver-based zonal velocity estimates.

7. Summary and Concluding Remarks

[49] The analytical relationship between the scintillation pattern velocity, the irregularities' velocity and position, and the satellite velocity has been derived. This relationship is consistent with previous works, and succinctly illustrates effects of satellite motion and magnetic field direction on the scintillation pattern velocity.

[50] Two different methods of estimating the zonal irregularity velocity were presented. The first uses a geostationary satellite and an appropriate satellite and receiver geometry to minimize the mapping of the vertical irregularity velocity. This method can estimate the instantaneous zonal irregularity velocity. The second method involves estimating the average zonal irregularity velocity using numerous GPS satellites. The averaging reduces the effect of the vertical irregularity velocity and deemphasizes the use of an assumed mean scattering height.

[51] The average zonal irregularity velocity has been computed for a 3-week period in March 2002 at São Luís, Brazil. This velocity compares well with climatological

results from Jicamarca Radio Observatory and illustrates that the average zonal velocity can be estimated using the GPS constellation.

Appendix A: Derivation of the Scintillation Pattern Velocity Equation

[52] The scintillation pattern velocity equation defined here is the relationship between the scintillation pattern velocity, the irregularities' position and velocity, and the satellite position and velocity. Its general form is derived for an arbitrary satellite and receiver geometry. The satellite is allowed to move, while it is assumed that the receiver is stationary. An implied assumption is that the satellite and receiver are both far enough from the irregularities such that scintillations can develop. This is the Huygens-Fresnel diffraction criteria.

[53] Refractive effects on the radio wave are ignored. Typical frequencies of radio wave sources span a range from hundreds of MHz to tens of GHz, which are much greater than the plasma frequency or ion and electron gyrofrequencies.

[54] The receiver coordinate system is shown in Figure 1. This coordinate system has its x axis aligned along the magnetic eastward (zonal) direction and its z axis coincides with the local vertical direction. The y axis completes the right-hand coordinate system.

[55] The plane containing the ionospheric puncture point to satellite vector, $\vec{r}_{ionsat}$, and the magnetic field unit vector, $\hat{B}$, at the ionospheric puncture point is denoted the projection plane. The irregularities, which are aligned along the magnetic field lines, produce a scintillation pattern that is projected onto the receiver plane.

[56] Specifying an infinitesimally thin plane is an approximation. This assumes that the receivers can precisely measure the scintillation pattern velocity. Measurement noise from receiver noise, decorrelation effects, and multipath can be minimized by choosing a longer data time span used to compute cross correlations.

[57] The equation for the projection plane in general geometric form is

$$\vec{q}^{\,\mathsf{T}}(\vec{r}-\vec{r}_{ion})=0, \tag{A1}$$

where $\vec{q}$ is the normal vector to the plane at the ionospheric puncture point, $\vec{r}_{ion}=(x_{ion},y_{ion},z_{ion})^{\mathsf{T}}$ is the position of the ionospheric puncture point, $\vec{r}$ is another point in the plane, and the superscript T represents a vector transpose. All vectors are 3×1 column vectors. $\vec{q}$ can be written as

$$\vec{q}=\hat{B}(\vec{r}_{ion})\times\vec{r}_{ionsat}, \tag{A2}$$

where $\hat{B}(\vec{r}_{ion})$ is the magnetic field unit vector at the ionospheric puncture point and $\vec{r}_{ionsat}$ is the vector from the ionospheric puncture point to the satellite. Note that the magnitudes of $\hat{B}(\vec{r}_{ion})$ and $\vec{r}_{ionsat}$ do not matter, only their direction.

[58] The intersection of the projection plane and the receiver plane represents the projection of the scintillation pattern onto the receiver plane. The velocity of this intersecting line can be found by differentiating equation (A1) with respect to time:

$$\frac{\partial}{\partial t}\left[\vec{q}^{\,\mathsf{T}}(\vec{r}-\vec{r}_{ion})\right]=0. \tag{A3}$$

[59] Since the zonal irregularity velocity is typically of interest, equation (A3) is expanded, placing the zonal, meridional, and vertical scintillation pattern velocities on the left hand side:

$$\begin{aligned}\frac{\partial r_x}{\partial t}+\frac{q_y}{q_x}\frac{\partial r_y}{\partial t}+\frac{q_z}{q_x}\frac{\partial r_z}{\partial t}=\frac{\partial r_{ionx}}{\partial t}+\frac{q_y}{q_x}\frac{\partial r_{iony}}{\partial t}+\frac{q_z}{q_x}\frac{\partial r_{ionz}}{\partial t}\\ -\frac{\partial q_x}{\partial t}\frac{(r_x-r_{ionx})}{q_x}\\ -\frac{\partial q_y}{\partial t}\frac{(r_y-r_{iony})}{q_x}\\ -\frac{\partial q_z}{\partial t}\frac{(r_z-r_{ionz})}{q_x}.\end{aligned} \tag{A4}$$

[60] Equation (A4) is exact, but not necessarily useful in its current form. A more easily interpretable definition of the zonal scintillation pattern velocity in the receiver plane can be found by substitution and simplification. Substitution is made using the following:

$$\vec{r}_{rec}=(x_{rec},y_{rec},0)^{\mathsf{T}}, \tag{A5}$$

$$\vec{r}_{ion}=(x_{ion},y_{ion},z_{ion})^{\mathsf{T}}, \tag{A6}$$

$$\vec{r}=\vec{r}_{rec}, \tag{A7}$$

along with the components of $\vec{q}$. With these substitutions, equation (A4) simplifies to

$$\begin{aligned}v_{scintx}=\frac{z_{sat}}{z_{sat}-z_{ion}}\Big\{v_{ionx}+(q_y/q_x)v_{iony}\\ +(q_z/q_x)v_{ionz}-\frac{z_{ion}}{z_{sat}}\Big[v_{satx}+(q_y/q_x)v_{saty}\\ +(q_z/q_x)v_{satz}\Big]\Big\},\end{aligned} \tag{A8}$$

where v_{scintx} is the measured zonal scintillation pattern velocity, z_{sat} is the satellite height, z_{ion} is the mean ionospheric puncture point height, v_{ionx} is the mean zonal irregularity velocity, v_{iony} is the mean meridional irregularity velocity, v_{ionz} is the mean vertical irregularity velocity, and $\vec{v}_{sat}$ is the satellite velocity. The partial time derivative of equation (A6) is the irregularities' velocity at the ionospheric puncture point. The partial time derivative of equation (A7) is the velocity of the intersection of the projection plane at the receiver's position. Note that it has also been assumed that $|\vec{r}_{rec}|\ll z_{sat}$ and $|\vec{r}_{rec}|\ll z_{ion}$.

[61] A more compact form of equation (A8) is

$$v_{scintx} = \frac{z_{sat}}{q_x(z_{sat} - z_{ion})} \left\{ \vec{q}^{\,\mathsf{T}} \vec{v}_{ion} - \frac{z_{ion}}{z_{sat}} \left[\vec{q}^{\,\mathsf{T}} \vec{v}_{sat} \right] \right\}. \tag{A9}$$

[62] Note that equation (A8) is similar to equation (15) of *Costa et al.* [1988], except that the magnetic field direction, meridional irregularity velocity, and meridional and vertical satellite velocity are accounted for here. It is interesting to note that their derivation was a consequence of the functional form of the scintillation pattern correlation function and its relationship to the irregularity correlation function.

[63] The ratios of normal vector components, q_y/q_x and q_z/q_x, are given by

$$\frac{q_y}{q_x} = \frac{B_z/B_y \tan(\phi) \sin(\theta) - B_x/B_y}{1 - B_z/B_y \tan(\phi) \cos(\theta)}, \tag{A10}$$

$$\frac{q_z}{q_x} = \frac{-\tan(\phi) \sin(\theta) + B_x/B_y \tan(\phi) \cos(\theta)}{1 - B_z/B_y \tan(\phi) \cos(\theta)}, \tag{A11}$$

where ϕ is the satellite zenith angle, θ is the satellite azimuth angle from magnetic north, and B_z/B_y and B_x/B_y are ratios of the components of the magnetic field unit vector at the ionospheric puncture point.

[64] The scintillation pattern is projected onto the receiver plane at an angle with respect to the magnetic meridian. This projection is analogous to a flagpole's shadow cast on the ground by the sun. The orientation of the shadow depends on two variables. First, it rotates as the sun moves across the sky. Second, the shadow's orientation depends on the flagpole's tilt with respect to the ground. In this example, the sun is a satellite and the flagpole's tilt is the direction of the magnetic field at the ionospheric puncture point.

[65] The projection angle in the receiver plane, θ_{projxy}, is given by

$$\theta_{projxy} = \arctan\left(\frac{-q_y}{q_x}\right) = \arctan\left[\frac{-B_z/B_y \tan(\phi) \sin(\theta) + B_x/B_y}{1 - B_z/B_y \tan(\phi) \cos(\theta)}\right]. \tag{A12}$$

[66] Simplifying this equation using the magnetic field vector at the origin of the receiver coordinate system gives the following:

$$\theta_{projxy} = \arctan\left[\frac{-\tan(\psi_{dip}) \tan(\phi) \sin(\theta)}{1 - \tan(\psi_{dip}) \tan(\phi) \cos(\theta)}\right], \tag{A13}$$

where ψ_{dip} is the magnetic dip angle. Equation (A13) is equivalent to equation (4) of *Kintner et al.* [2004]. Note that they used a different method to derive the projection angle which only involved trigonometry.

[67] The projection angle in the *xz* plane is equal to

$$\theta_{projxz} = \arctan\left(\frac{-q_z}{q_x}\right) = \arctan\left[\frac{\tan(\phi) \sin(\theta) - B_x/B_y \tan(\phi) \cos(\theta)}{1 - B_z/B_y \tan(\phi) \cos(\theta)}\right]. \tag{A14}$$

[68] The zonal scintillation pattern velocity, v_{scintx}, is defined as

$$v_{scintx} = v_x + (q_y/q_x)v_y + (q_z/q_x)v_z \tag{A15}$$

The fact that the zonal, meridional, and vertical scintillation pattern velocities are coupled is not a significant problem. The measured velocity in the zonal direction is equal to the sum of these velocities in equation (A15). This is a consequence of the long correlation distance along the projection and the large signal propagation speed, which make a zonal scintillation pattern drift indistinguishable from a meridional or vertical drift.

[69] **Acknowledgments.** This work has been supported in part by ONR grant N00014-92-J-1822.

[70] Arthur Richmond thanks H. Kil and Cesar E. Valladares for their assistance in evaluating this paper.

References

Aggson, T. L., N. C. Maynard, F. Herrero, H. G. Mayr, L. Brace, and M. Liebrecht (1987), Geomagnetic equatorial anomaly in zonal plasma flow, *J. Geophys. Res.*, *92*(A1), 311–315.

Anderson, D. N., and M. Mendillo (1983), Ionospheric conditions affecting the evolution of equatorial plasma depletions, *Geophys. Res. Lett.*, *10*(7), 541–544.

Basu, S., S. Basu, E. Kudeki, H. P. Zeningonul, M. A. Biondi, and J. W. Meriwether (1991), Zonal irregularity drifts and neutral winds measured near the magnetic equator in Peru, *J. Atmos. Terr. Phys.*, *53*(8), 743–755.

Basu, S., et al. (1996), Scintillations, plasma drifts, and neutral winds in the equatorial ionosphere after sunset, *J. Geophys. Res.*, *101*(A12), 26,795–26,809.

Beach, T. L., and P. M. Kintner (2001), Development and use of a GPS ionospheric scintillation monitor, *IEEE Trans. Geosci. Remote Sens.*, *39*(5), 918–928.

Bhattacharyya, A., S. Basu, K. M. Groves, C. E. Valladares, and R. Sheehan (2001), Dynamics of equatorial *F* region irregularities from spaced receiver scintillation observations, *Geophys. Res. Lett.*, *28*(1), 119–122.

Briggs, B. H., G. J. Phillips, and D. H. Shinn (1950), The analysis of observations on spaced receivers on the fading of radio signals, *Proc. Phys. Soc. London, Sect. B*, *63*, 106–121.

Briggs, B. H., G. J. Phillips, and D. H. Shinn (1968), On the analysis of moving patterns in geophysics, I. Correlation analysis, *J. Atmos. Terr. Phys.*, *30*, 1777–1788.

Costa, E., and P. F. Fougere (1988), Cross-analysis of spaced-receiver measurements, *Radio Sci.*, *23*(2), 129–139.

Costa, E., P. F. Fougere, and S. Basu (1988), Cross-correlation analysis and interpretation of spaced-receiver measurements, *Radio Sci.*, *23*(2), 141–162.

Fejer, B. G., D. T. Farley, C. Gonzales, R. Woodman, and C. Calderon (1981), *F*-region east-west drifts at Jicamarca, *J. Geophys. Res.*, *86*(A1), 215–218.

Groves, K. M., et al. (1997), Equatorial scintillation and system support, *Radio Sci.*, *32*(5), 2047–2064.

Hofmann-Wellenhof, B., H. Lichtenegger, and J. Collins (1994), *GPS Theory and Practice*, Springer-Verlag, New York.

Karasawa, Y., K. Yasukawa, and M. Yamada (1985), Ionospheric scintillation measurements at 1.5 GHz in mid-latitude region, *Radio Sci.*, *20*(3), 643–651.

Kil, H., P. M. Kintner, E. R. de Paula, and I. J. Kantor (2000), Global Positioning System measurements of the ionospheric zonal apparent

velocity at Cachoeira Paulista in Brazil, *J. Geophys. Res.*, *105*(A3), 5317–5327.

Kil, H., P. M. Kintner, E. R. de Paula, and I. J. Kantor (2002), Latitudinal variations of scintillation activity and zonal plasma drifts in South America, *Radio Sci.*, *37*(1), 1006, doi:10.1029/2001RS002468.

Kintner, P. M., B. M. Ledvina, E. R. de Paula, and I. J. Kantor (2004), The size, shape, orientation, speed, and duration of GPS equatorial anomaly scintillations, *Radio Sci.*, *39*, RS2012, doi:10.1029/2003RS002878.

Livingston, R., C. Rino, J. Owen, and R. Tsunoda (1982), The anisotropy of high-latitude nighttime *F* region irregularities, *J. Geophys. Res.*, *87*(A12), 10,519–10,526.

Pingree, J. E., and B. G. Fejer (1987), On the height variation of the equatorial *F* region vertical plasma drifts, *J. Geophys. Res.*, *92*(A5), 4763–4766.

Ramo Rao, P. V. S., B. V. Ramana Rao, and D. S. V. V. D. Prasad (2000), A study on the zonal movements of ionospheric irregularities using two simulataneous geostationary satellite signals, *Indian J. Radio Space Phys.*, *29*(2), 66–70.

Rino, C. L., and R. C. Livingston (1982), On the analysis and interpretation of spaced-receiver measurements of transionospheric radio waves, *Radio Sci.*, *17*(4), 845–854.

Spatz, D. E., S. J. Franke, and K. C. Yeh (1988), Analysis and interpretation of spaced receiver scintillation data recorded at an equatorial station, *Radio Sci.*, *23*(3), 347–361.

Vacchione, J. D., S. J. Franke, and K. C. Yeh (1987), A new analysis technique for estimating zonal irregularity drifts and variability in the equatorial *F* region using spaced receiver scintilation data, *Radio Sci.*, *22*(5), 745–756.

Valladares, C. E., R. Sheehan, S. Basu, H. Keunzler, and J. Espinoza (1996), The multi-instrumented studies of equatorial thermosphere aeronomy scintillation system: Climatology of zonal drifts, *J. Geophys. Res.*, *101*(A12), 26,839–26,850.

Wernik, A. W., C. H. Liu, and K. C. Yeh (1983), Modeling of spaced-receiver scintillation measurements, *Radio Sci.*, *18*(5), 743–764.

Yeh, K. C., and C. H. Liu (1982), Radio wave scintillations in the ionosphere, *Proc. IEEE*, *70*(4), 324–360.

E. R. de Paula, Aeronomy Division-DAE/CEA, INPE, São José dos Campos, São Paulo, Brazil. (eurico@dae.inpe.br)

P. M. Kintner and B. M. Ledvina, School of Electrical and Computer Engineering, Cornell University, Ithaca, NY 14853, USA. (bml22@cornell.edu; pmk1@cornell.edu)